Comparison of X-31 Flight, Wind-Tunnel, and Water-Tunnel Yawing Moment Asymmetries at High Angles of Attack

Brent R. Cobleigh
PRC Inc.
Edwards, California

Mark A. Croom
NASA Langley Research Center

B. F. Tamrat
Rockwell NAA

Fourth NASA High Alpha Conference
Edwards, California
July 12-14, 1994

94-152

N95-14234

Program and Vehicle Description

The X-31 aircraft are being used in the enhanced fighter maneuverability (EFM) research program, which is jointly funded by the (U.S.) Advanced Research Projects Agency (ARPA) and Germany's Federal Ministry of Defense (FMOD). The flight test portion of the program, which involves two aircraft, is being conducted by an International Test Organization (ITO) comprising the National Aeronautics and Space Administration (NASA), the U.S. Navy, the U.S. Air Force, Rockwell International, and Deutsche Aerospace (DASA). The goals of the flight program are to demonstrate EFM technologies, investigate close-in-combat exchange ratios, develop design requirements, build a database for application to future fighter aircraft, and develop and validate low-cost prototype concepts.

For longitudinal control the X-31 uses canards, symmetrical movement of the trailing-edge flaps, and pitch deflection of the thrust vectoring system. The trim, inertial coupling, and engine gyroscopic coupling compensation tasks are performed primarily by the trailing-edge flaps. For lateral-directional control the aircraft uses differential deflection of the trailing-edge flaps for roll coordination and a conventional rudder combined with the thrust vectoring system to provide yaw control. The rudder is only effective up to about 40° angle of attack (α), after which the thrust vectoring becomes the primary yaw control effector. Both the leading-edge flaps and the inlet lip are scheduled with the angle of attack to provide best performance.

Comparison of X-31 Flight, Wind-Tunnel, and Water-Tunnel Yawing Moment Asymmetries at High Angles of Attack

Brent R. Cobleigh
PRC Inc.
Edwards, California

Mark A. Croom
NASA Langley Research Center
B. F. Tamrat
Rockwell NAA

Fourth NASA High Alpha Conference
Edwards, California
July 12-14, 1994

94-152

Nomenclature

AB	afterburner
C_d	drag force coefficient
C_n	yawing moment coefficient
C_Y	side force coefficient
d	body diameter
EFM	enhanced fighter maneuverability
FB	forebody
g	aircraft normal load factor
KCAS	knots calibrated airspeed
l	body length
L	characteristic length
M	Mach number
NB	noseboom
$qbar$	dynamic pressure, lb/ft^2
Re	Reynolds number, $\rho L V/\mu$
S1	20-in. long by .60-in. wide strake
S2	47-in. long by .60-in. wide strake
V	velocity
α	angle of attack, deg
β	sideslip angle, deg
μ	dynamic viscosity
ρ	density

Subscripts

d	based on noseboom diameter of 3.5 in.
D	based on forebody base diameter of 3.2 ft
max	maximum
0	at zero sideslip angle

D R Y D E N F L I G H T

Outline

- **Background**

- **Flight history**

- **Analysis method**

- **Results**
  - **Flight test**
  - **Comparison with wind tunnel**
  - **Comparison with water tunnel**

- **Conclusions**
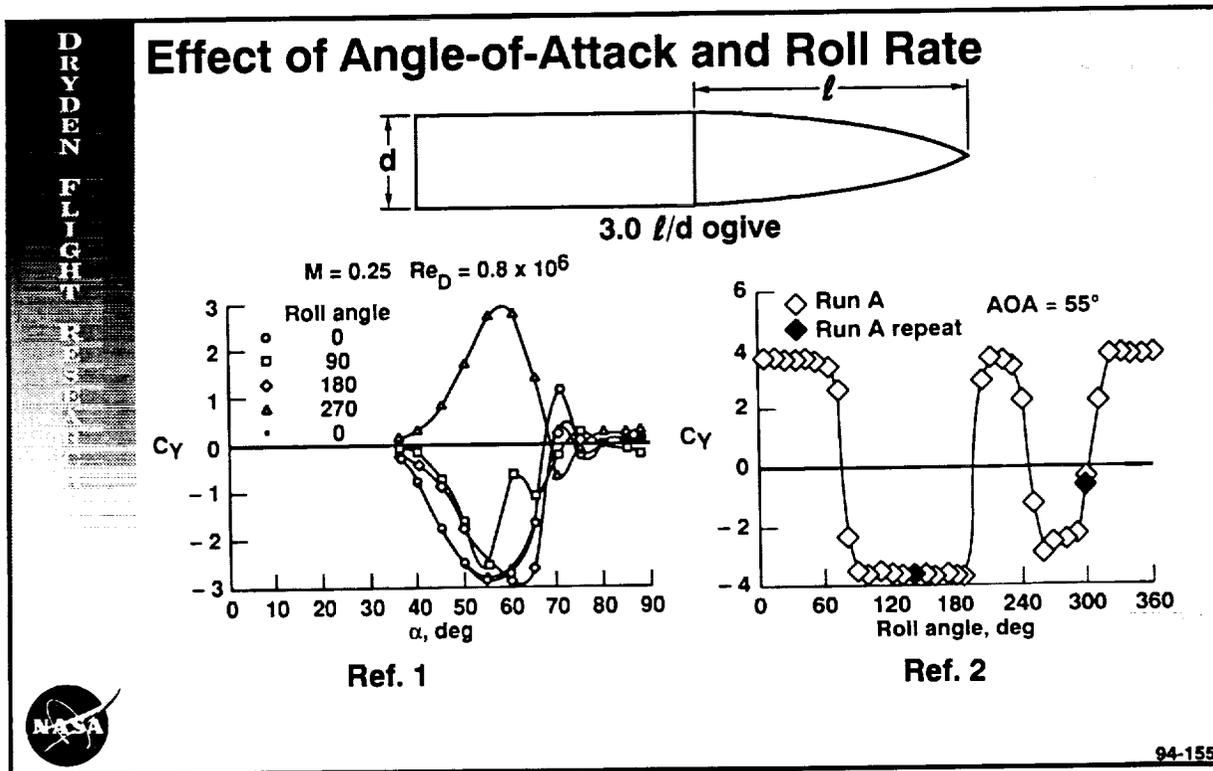
- **Current status**

94-153

Generic High-Angle-of-Attack Asymmetry

The long slender forebody shapes of modern fighter aircraft make them susceptible to the body side-force phenomena. This side force is the result of surface pressure imbalances around the forebody of the aircraft caused by an asymmetric forebody boundary layer and vortex system at high angles of attack. In this scenario, the boundary layer on each side of the forebody separates at different locations as shown in the figure. At separation, corresponding vortex sheets are generated that roll up into an asymmetrically positioned vortex pair. The forces on the forebody are generated primarily by the boundary layer and to a lesser extent by the vortices, depending on their proximity to the forebody surface. The figure shows a typical asymmetrical arrangement where the lower, more inboard vortex corresponds to a boundary layer that separated later and, the higher, more outboard vortex corresponds to the boundary layer that separated earlier. The suction generated by the more persistent boundary layer and the closer vortex combine to create a net force in their direction. Since the center of gravity of the aircraft is well aft of the forebody, a sizable yawing moment asymmetry develops.

Generic High-Angle-of-Attack Asymmetry
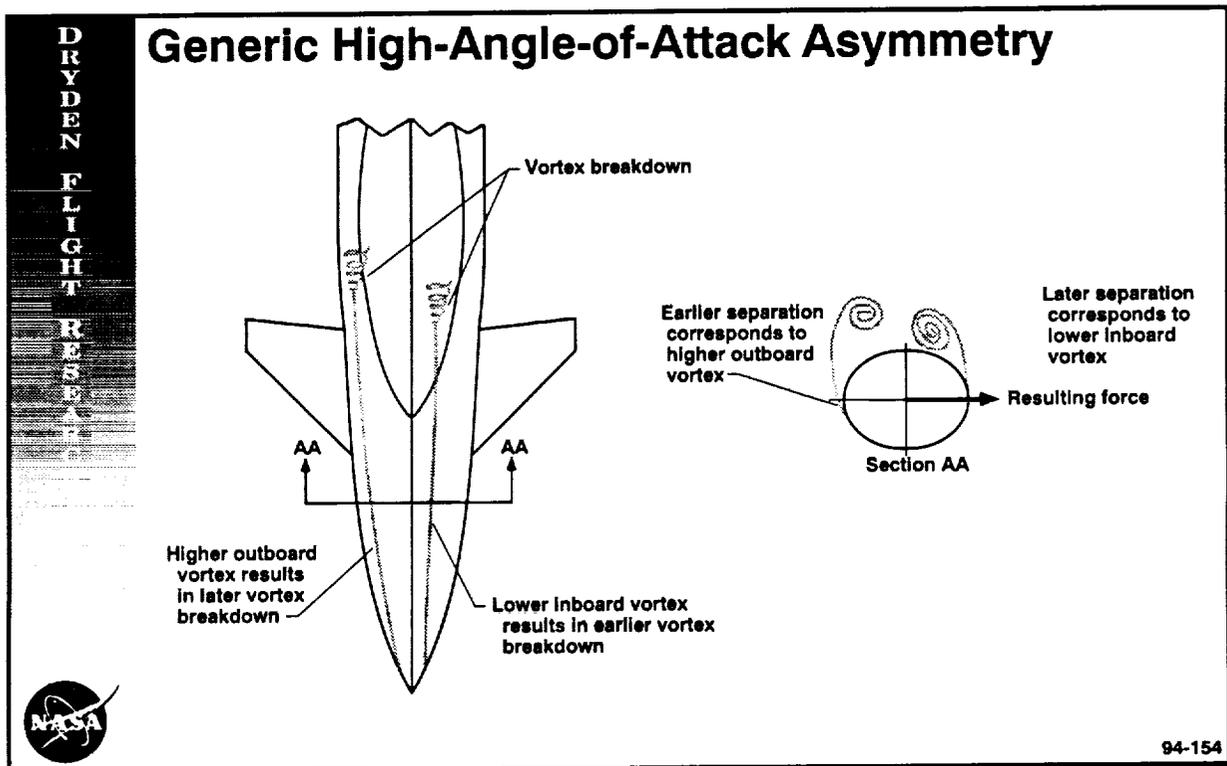
Effect of Angle of Attack and Roll Angle

An illustration of the asymmetry problem was shown by measuring the side force on an axisymmetric body at different roll angles at a given angle of attack. Because the model is axisymmetric, no lateral-directional forces or moments would be expected. The left plot (ref. 1), however, shows that a large asymmetry develops on a 3.0 l/d fineness ratio ogive model starting at approximately $\alpha = 35°$, that continues up past $\alpha = 70°$. In addition the sign of the asymmetry switches for a roll angle of 270°. Further tests by other researchers confirmed that the magnitude of the largest asymmetry does not change smoothly with changing roll angle (right plot, ref. 2). Instead, as the ogive cylinder is rolled through 360°, four changes in the sign of the asymmetry occur. Thus, at high angles of attack, the vortex cores can have bi-stable states, neither of which is symmetric. Other tests have shown that rotation of the nosetip alone produces the same result, suggesting that micro-asymmetries near the model tip are significant in the asymmetry formation. [1,3,4,5]

Effect of Angle-of-Attack and Roll Rate

3.0 l/d ogive

$M = 0.25 \quad Re_D = 0.8 \times 10^6$

Roll angle
o	0
□	90
◇	180
▲	270
•	0

C_Y vs α, deg

Ref. 1

Run A
Run A repeat
AOA = 55°

C_Y vs Roll angle, deg

Ref. 2
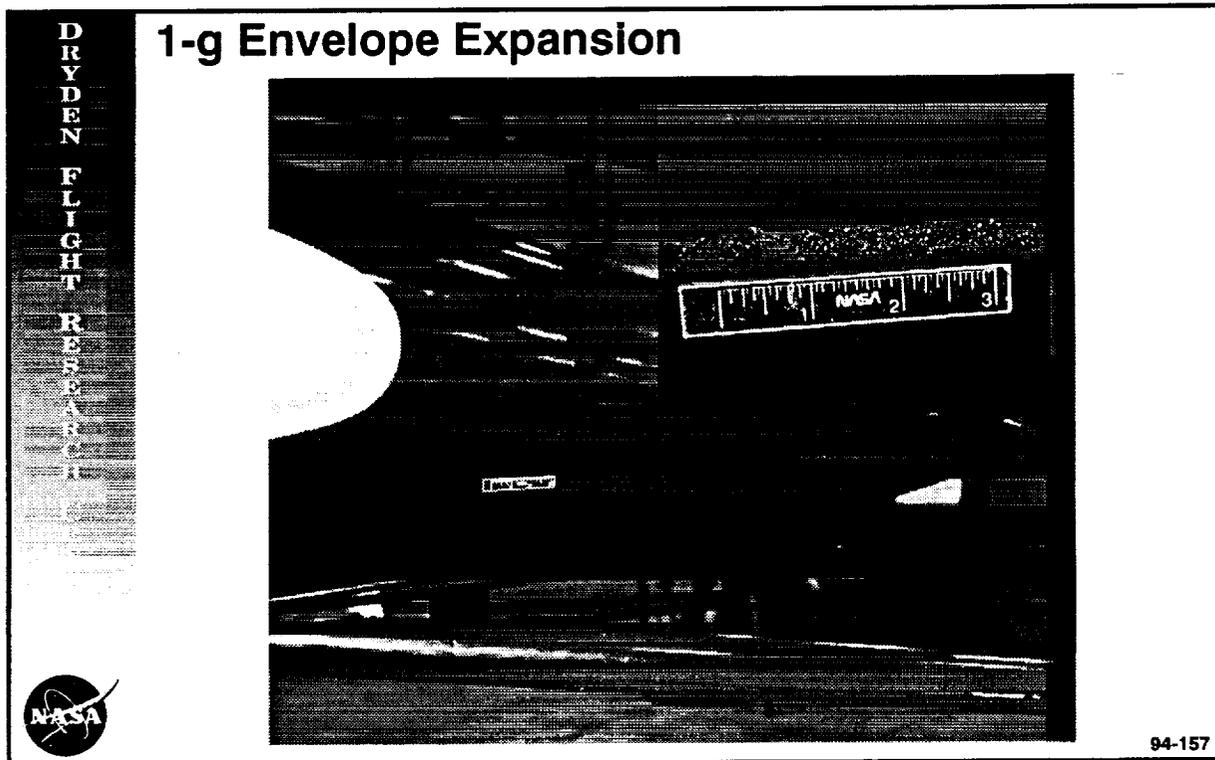
94-155

Effect of Reynolds Number

Reynolds number has also been shown to affect the asymmetry characteristic of slender bodies. The left plot (ref. 1) shows that large changes in the magnitude and sign of the asymmetry can be affected by Reynolds number; however, the angle-of-attack range over which the aircraft is susceptible to asymmetries remains unchanged. The nature of the boundary-layer separation on the forebody—whether it be laminar, transitional, or fully turbulent—is dependent on the Reynolds number. Above $\alpha = 30°$, the maximum side force on a 3.5 l/d ogive is significantly larger for laminar and turbulent separation conditions than it is with transitional flow (right plot, ref. 6). This Reynolds number effect is important when comparing flight derived asymmetry information with either wind-tunnel or water-tunnel data.

Effect of Reynolds Number

3.5 ℓ/d ogive
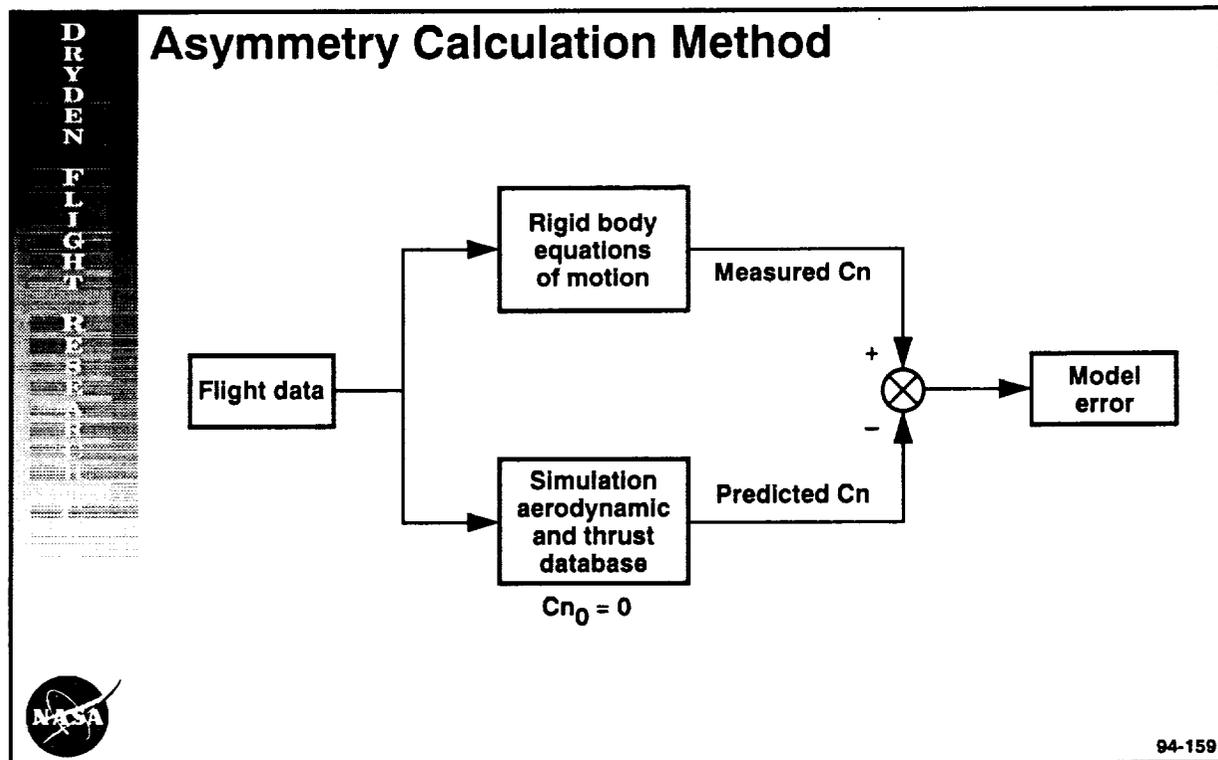
Ref. 1

Ref. 6

94-156
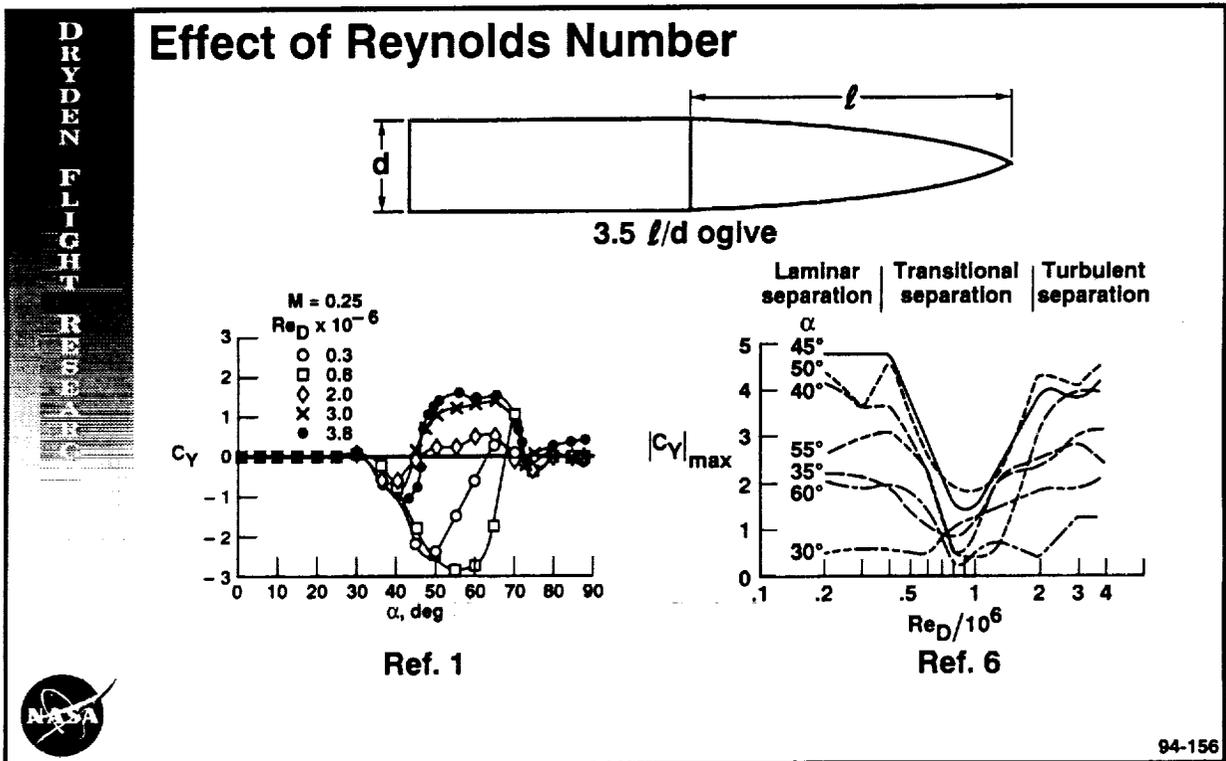
1-g Envelope Expansion

During the 1-g, high-α envelope expansion of the X-31, both test aircraft exhibited significant, but different, yawing moment asymmetries at 0° sideslip above α = 40°. Among the resulting aircraft responses were slow rolloffs and "lurches" (small, sharp heading changes). Although pilot compensation was attainable, up to 50 percent of roll stick deflection was required to counter the asymmetry. As a result the full-stick velocity vector roll rate of each aircraft was found to be faster in the direction of the asymmetry at a given angle of attack. To coordinate maneuvering with the yawing moment asymmetries, the control system had to increase the amount of control deflection required. In many cases this increase resulted in a position saturation of one of the trailing-edge flaps or thrust vector paddles.

To reduce the asymmetry, transition grit strips were applied along the forebody to force boundary-layer transition at the same location on both sides of the forebody. This method had shown some promise in reducing high-α yawing asymmetries during earlier tests on the F-18 High Alpha Research Vehicle (HARV).[7] Transition strips were also installed along the noseboom in the hope that a turbulent separation from the cylindrical cross-section would result in a reduced wake impinging on the forebody. These configuration changes improved the pilot-reported handling qualities somewhat; however, the asymmetries were not eliminated. The transition devices allowed the flight testing to complete the 1-g maneuvering envelope expansion of the X-31 successfully out to α = 70°.

DRYDEN FLIGHT RESEARCH

1-g Envelope Expansion

94-157

Elevated-*g* Expansion

Shortly into the high-α, elevated-*g* phase of the envelope expansion, a departure from controlled flight occurred on ship 2 as the pilot was performing a 2-*g* split-S maneuver to α = 60°. Data analysis showed that a large yawing moment, in excess of the available control power, had triggered the departure (left figure). Again the forebody vortex system was suspected to be the moment generator. An effort was begun to design and test forebody strakes with the intent of improving the forebody vortex symmetry by eliminating the large-amplitude flow asymmetries that caused the departure. Towards this goal a wind-tunnel test was conducted in the NASA Langley Research Center's 30-FT by 60-FT Tunnel to define the strake design and document the impact of the strake on the static aerodynamics.

The tests showed that strakes positioned longitudinally along the waterline of the forebody from the nosetip reduced the model yawing moment asymmetry. The effectiveness of the strakes at reducing the asymmetry was not a function of the strake width, although the length of the strakes affected the amount of undesirable nose-up pitching moment. Based on the wind-tunnel results, two different length strake sets were evaluated in flight. A 20-in. and a 46-in. long strake design were manufactured and then were flight tested in separate tests. Both strakes were 0.60-in. wide. The radius of the X-31 radome tip was rounded to a 1.2-in. diameter simultaneously with the strake installation.

Elevated-g Expansion

Asymmetry Calculation Method

To better understand and quantify the high-angle-of-attack yawing moment asymmetry characteristic of the X-31 aircraft, a method was developed to calculate time histories of the asymmetric forces and moments on the aircraft from flight data.[8] The figure shows a block diagram of the method. The flight-measured yawing moment was computed by substituting the flight-measured variables into the rigid body equation of motion. The flight-measured yawing moment was then subtracted from that predicted from the simulation aerodynamic and thrust databases to calculate the missing, unmodeled components. By restricting data analysis to symmetrical maneuvers in which sideslip, roll rate, and yaw rate were small, the cause of the missing aerodynamic yawing moment was narrowed to three main sources: (1) errors in the thrust vectoring model, (2) errors in the control effectiveness model, and (3) aerodynamic asymmetries. Because the control effectiveness database was verified and updated with parameter identification results and the thrust model errors were not expected to be a strong function of angle of attack, any changes in the missing components with increases in angle of attack were attributed to aerodynamic asymmetries. An analysis of multiple decelerations, pullups, and split-S maneuvers with the same aircraft configuration resulted in a "fingerprint" of the asymmetry characteristic for a given configuration at a given flight condition.
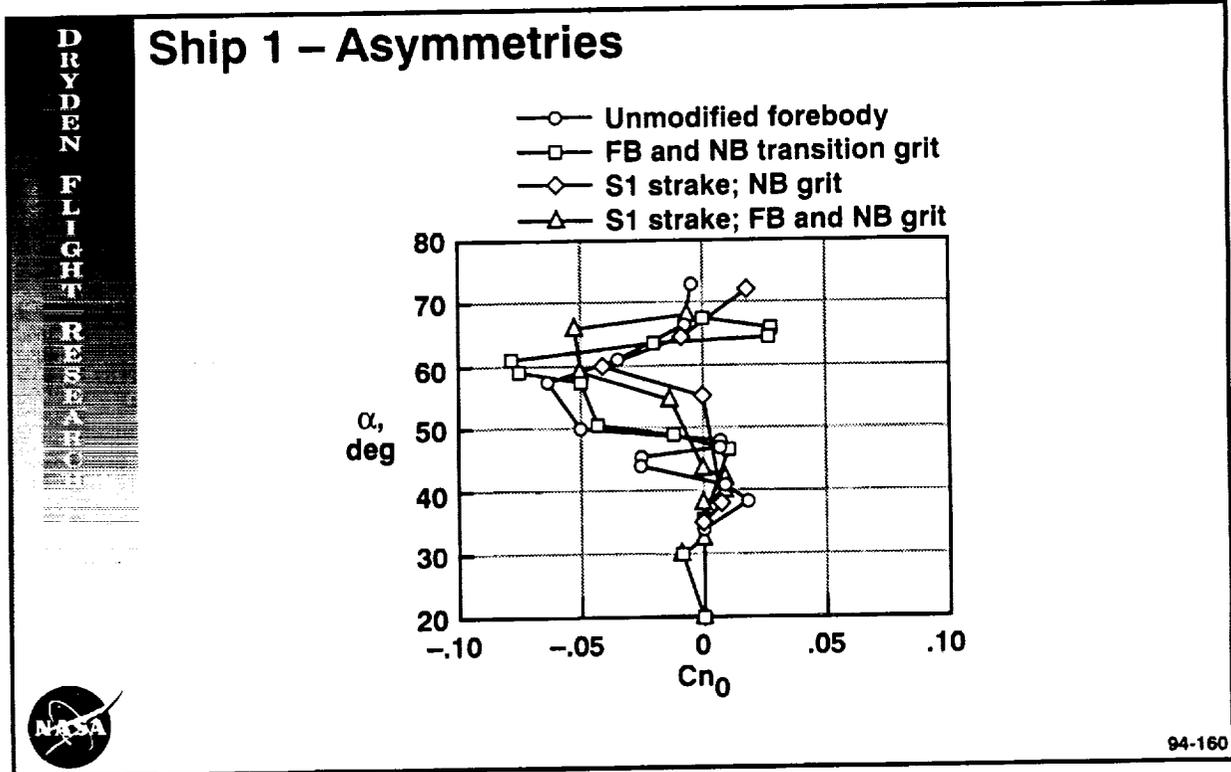

DRYDEN FLIGHT RESEARCH CENTER

Asymmetry Calculation Method

Flight data → Rigid body equations of motion → Measured Cn (+)

Flight data → Simulation aerodynamic and thrust database → Predicted Cn (−)

$Cn_0 = 0$

⊗ → Model error

94-159

Ship 1 Asymmetries

The figure shows yawing moment asymmetry for ship 1 during slow (essentially 1-g) decelerations to high-α conditions for several of the flight configurations. The largest asymmetry started to build up beginning at $\alpha = 48°$ to a peak of $C_{n0} = -0.063$ at approximately $\alpha = 57°$. The asymmetry diminished significantly in magnitude by $\alpha = 66°$.

In response to these asymmetries a transition grit strip was installed on both sides of the forebody and along the sides of the noseboom. Unfortunately, the data as plotted in the figure indicate that the asymmetry problem was magnified. Although the largest asymmetry began to build at the same angle of attack (48°), the peak asymmetry increased to $C_{n0} = -0.078$. The addition of the transition strips increased the angle at which the largest asymmetry occurred from 58° to 61°.

The replacement of the forebody transition strip with the S1 strake, along with the blunting of the nosetip, effectively delayed the initiation of the yawing moment asymmetry up to an angle of attack of 55°. A peak asymmetry of $C_{n0} = -0.040$ occurred at $\alpha = 60°$, after which the asymmetry diminished. As with the unmodified forebody, the aircraft became nearly symmetric by $\alpha = 65°$.

The addition of a boundary-layer transition strip along the forebody aft of the strake resulted in an increase in the asymmetry level. A sharp change in the asymmetry occurred near $\alpha = 55°$. An asymmetry level of $C_{n0} \approx -0.050$ remained over a range of $\alpha = 59°$ to 66°. Thus, the addition of the forebody transition strip increased the yawing moment asymmetry and caused it to remain at its largest level for a broader angle-of-attack range.

Ship 1 – Asymmetries

—○— Unmodified forebody
—□— FB and NB transition grit
—◇— S1 strake; NB grit
—△— S1 strake; FB and NB grit

94-160

Ship 2 Asymmetries

The yawing moment asymmetry characteristic of ship 2 was significantly more troublesome than that of ship 1. As a result, greater effort was made to reduce the asymmetry on ship 2 through configuration changes. In addition to the configurations changes flown with ship 1, an extended length strake, S2, was also tested.
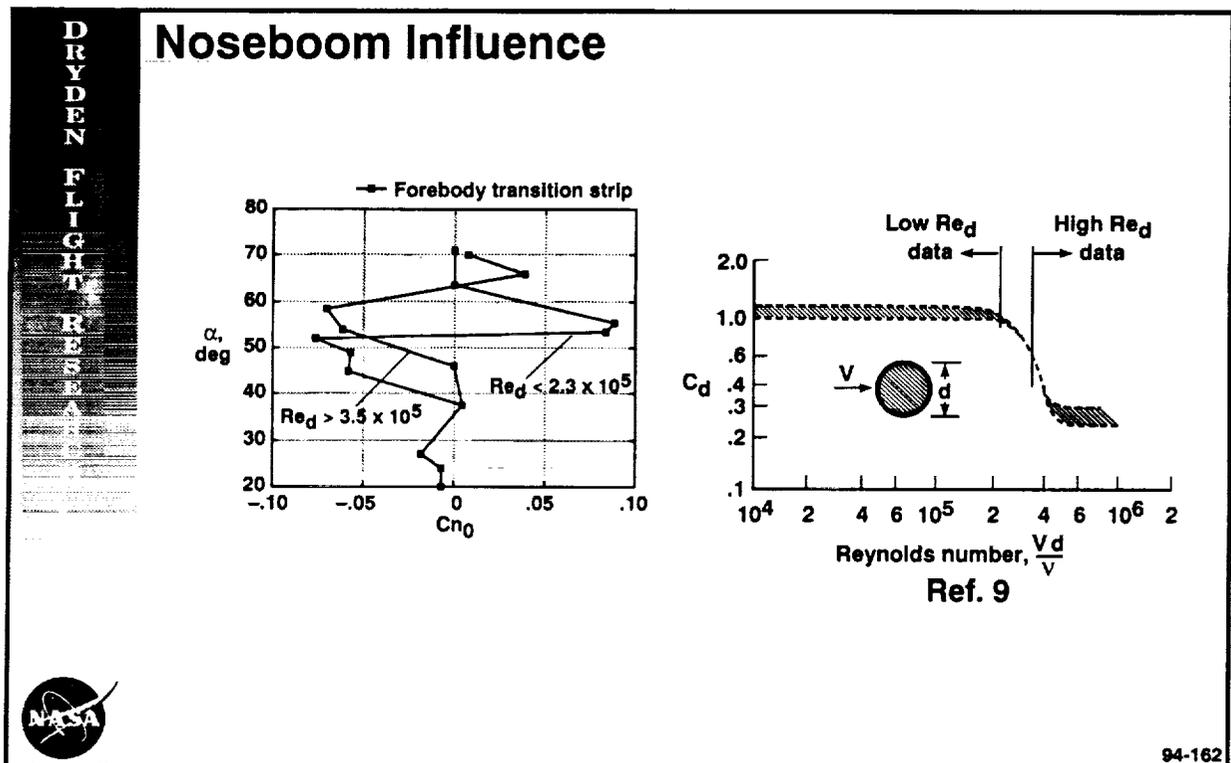
The asymmetry plot for the unmodified forebody during 1-g maneuvers did not show easily distinguishable trends in the asymmetry with angle of attack. Each maneuver appeared to have a random asymmetry pattern. Plots of the asymmetry range as a function of angle of attack (left figure) show that the maximum yawing moment asymmetry appears to be bounded at $|C_{n_0}| < 0.10$.

The addition of forebody and noseboom transition strips resulted in a more regular asymmetry characteristic than that for the unmodified forebody during 1-g decelerations; however, some scatter still existed about the average asymmetry. The figure plots the range of the scatter for this configuration. The asymmetry initially goes to the right to a peak of up to $C_{n_0} = 0.050$ at an angle of attack between 48° and 54°. As the angle increased, the asymmetry switched to the left, eventually reaching its maximum asymmetry near $\alpha = 67°$. The switching of the asymmetry from the right to left resulted in a change in the yawing moment of about $\Delta C_n \approx 0.10$.
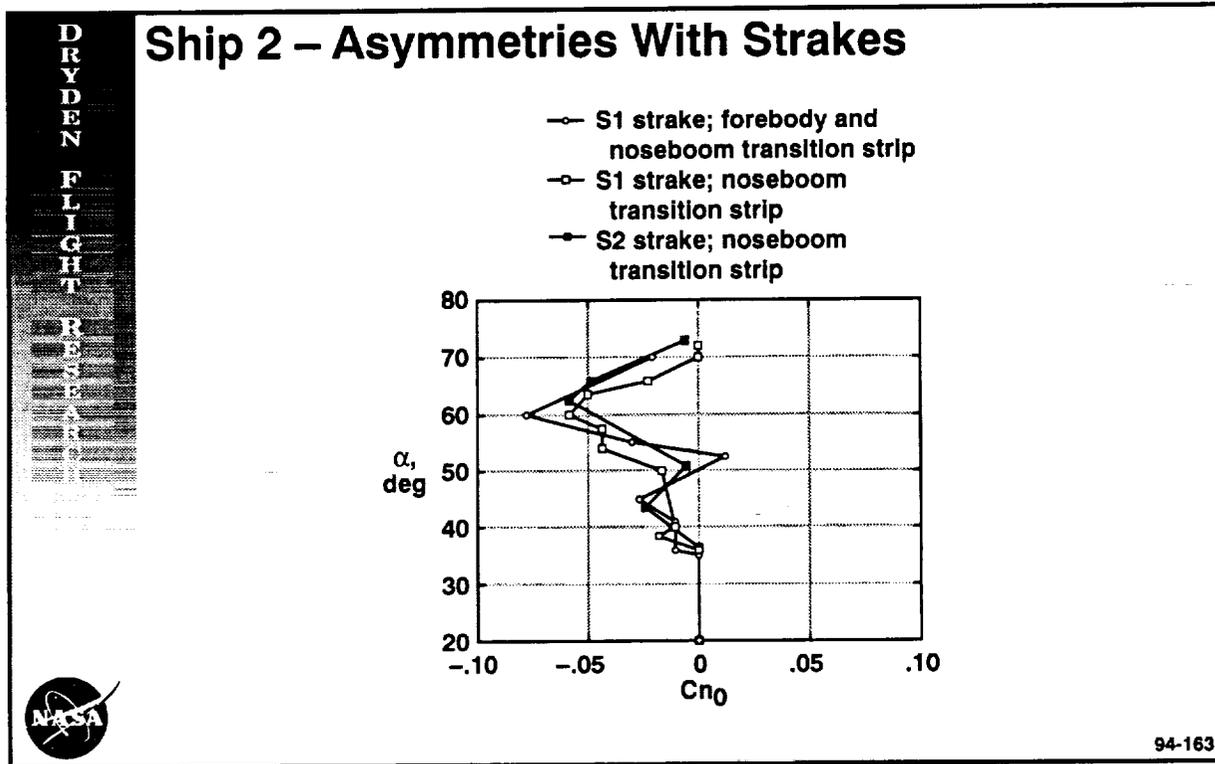

Ship 2 – Asymmetries
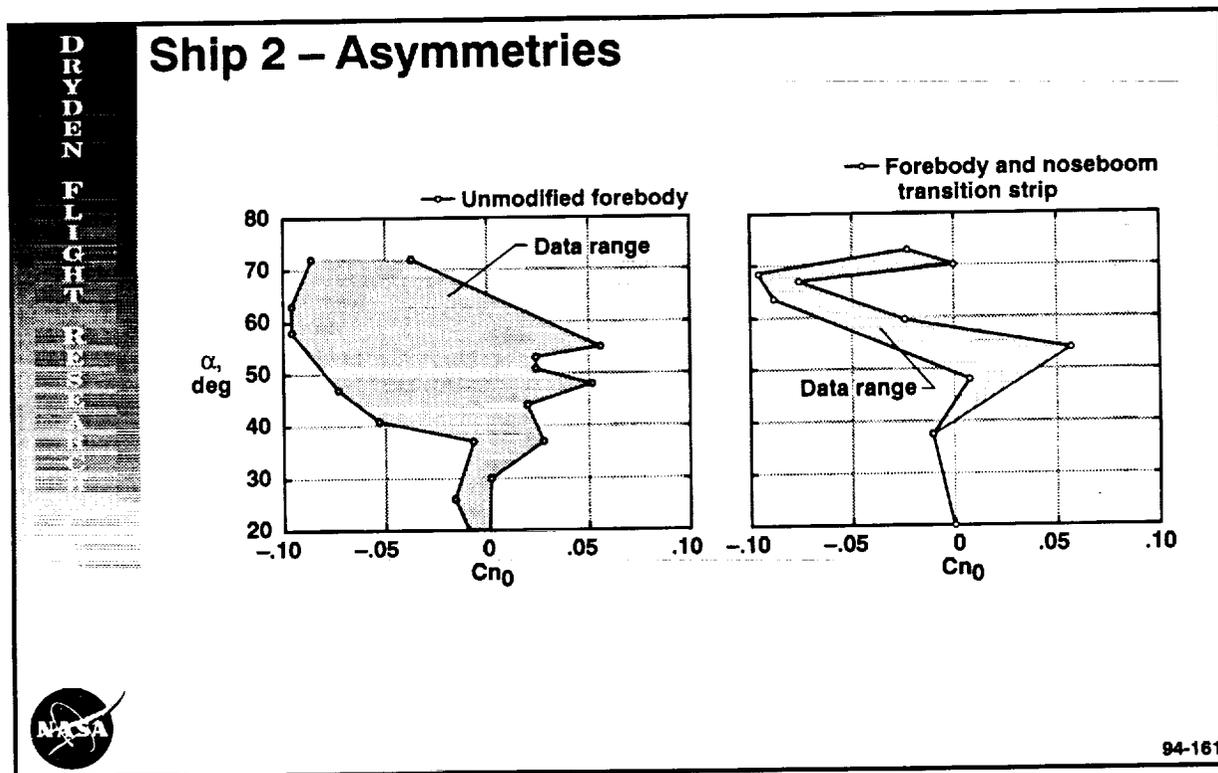
Noseboom Influence

The initial purpose of the noseboom transition strip was to ensure that the boundary layer on the flight test noseboom was turbulent before separation. It is well known that a turbulent boundary layer on a circular cylinder stays attached longer, thereby reducing the wake and resulting drag (right figure). Without the transition strip the separation state was subject to the local Reynolds number and noseboom roughness. The left figure shows that two different asymmetry characteristics developed on ship 2 when the noseboom transition strip was removed. Calculating the approximate Reynolds number based on noseboom diameter for each of the maneuvers showed that the two asymmetry characteristics occurred over different Reynolds-number ranges. Plotting both Reynolds-number ranges on a chart of the boundary-layer separation state of a circular cylinder as a function of Reynolds number (right figure) shows that a difference in the boundary-layer state at separation could have existed between the two sets of data. The lower Reynolds-number data, which would result in a large separation wake, had a sharp change in the asymmetry above $\alpha = 50°$ that built up to a large right asymmetry. On the other hand, the higher Reynolds-number flow, which would produce a smaller separation wake, had a milder buildup in asymmetry. The higher Reynolds-number data more closely matched the data with the noseboom transition strips installed, suggesting that the strip was successful in eliminating a laminar separation, as it was originally intended to do.

DRYDEN FLIGHT RESEA...

Noseboom Influence

Forebody transition strip

α, deg — Cn_0

$Re_d < 2.3 \times 10^5$

$Re_d > 3.5 \times 10^5$

Low Re_d data — High Re_d data

C_d

Reynolds number, $\dfrac{Vd}{v}$

Ref. 9

94-162

Ship 2 Asymmetries With Strakes

The first real improvement in the yawing moment asymmetries on ship 2 was found with the addition of forebody strakes and the blunting of the nosetip. The figure shows data from the S1 and S2 strake flight tests. The S1 strake, 1.0-in. diameter blunt nosetip, and noseboom transition strip combination resulted in a comparably slow buildup of asymmetry starting at approximately $\alpha = 50°$. The asymmetry reached a peak value of $C_{n0} = -0.059$ at $\alpha = 60°$. As with most other configurations the asymmetry diminished to near zero by $\alpha = 70°$. The addition of a transition strip aft of the S1 strake increased the maximum asymmetry from $C_{n0} = -0.059$ to -0.078. This increase was similar to that seen on ship 1. Because the 20-in. long S1 strake reduced the maximum yawing moment asymmetry level, a longer 46-in. strake, S2, was installed and flight tested with the blunt nosetip. Unfortunately, little change in the 1-g deceleration asymmetries resulted. The longer strake did shift the asymmetry to a higher angle of attack by approximately 2°.

Ship 2 – Asymmetries With Strakes

- S1 strake; forebody and noseboom transition strip
- S1 strake; noseboom transition strip
- S2 strake; noseboom transition strip

94-163

Dynamic Poststall Maneuvers

The figures present the asymmetries calculated during rapid pullups to high angle of attack for the S1 strake, blunted nose, and noseboom transition strip configuration. The data obtained from the steady-state decelerations are plotted along with the dynamic data for comparison. In general the asymmetry level during the dynamic maneuvers was less than or equal to the value seen in the 1-g maneuvers at the maximum asymmetry angle of attack (near 60°). This reduction in asymmetry level during the dynamic portion of the maneuver, however, was not entirely useful. As the aircraft reached its target angle of attack and the load factor decayed to unity, the asymmetry often built up to the steady-state value. Thus, the maximum asymmetry defined by the 1-g decelerations provided the worst-case levels for which the flight control system had to account. Although the dynamic maneuvers reduced the maximum asymmetry near $\alpha = 60°$, an increase in the asymmetry was seen at lower angles of attack near $\alpha = 45°$ to 50°. In addition the maximum asymmetry measured when capturing $\alpha = 50°$ on ship 2 increased with increasing aircraft velocity. Although the addition of the S2 strake did not appear to reduce the maximum asymmetry at $\alpha = 60°$, the tendency of the asymmetry to go right at $\alpha = 50°$ during dynamic maneuvers appeared to be significantly reduced.

Dynamic Poststall Maneuvers

94-164
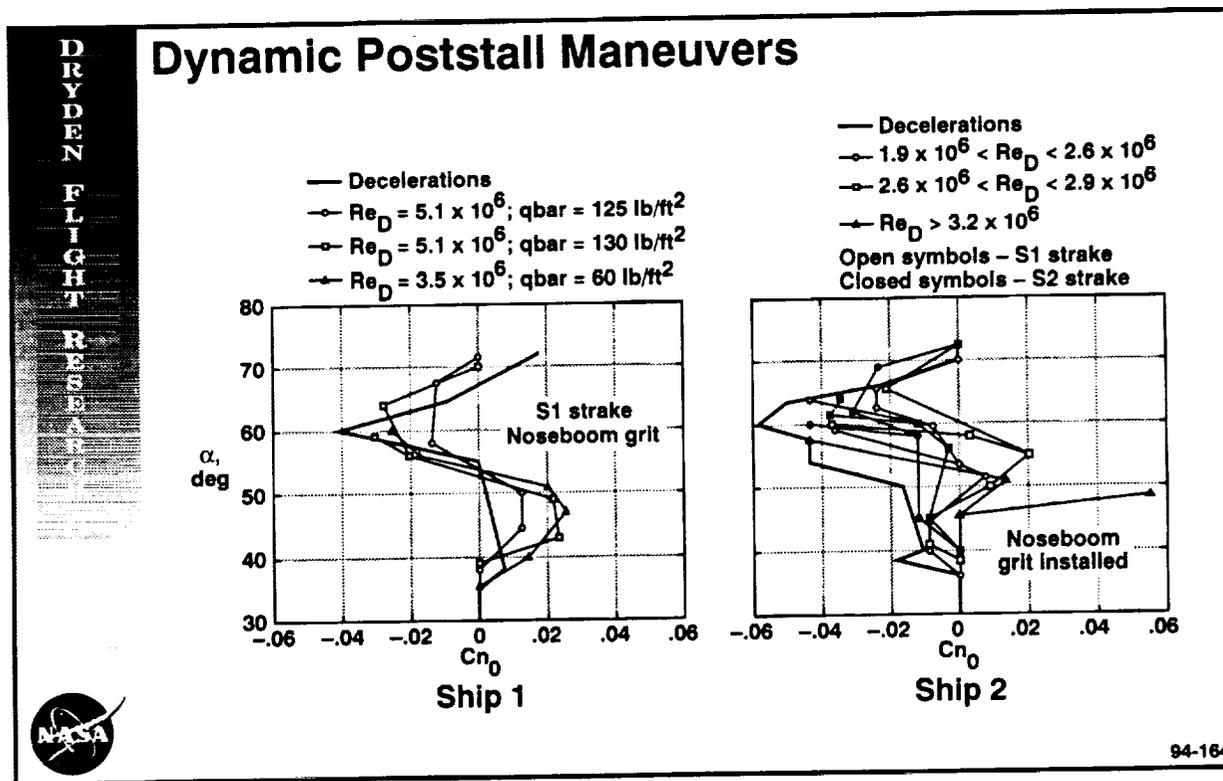
Comparison With Wind Tunnel

Although some yawing moment asymmetry was predicted in the wind tunnel at the high-α condition, the magnitude was significantly less than that seen in flight (left figure). One possible explanation has to do with Reynolds number. A plot of the asymmetry as a function of Reynolds number for an ogive (right figure) shows a significant decrease in the asymmetry at Reynolds numbers causing mixed boundary layer states on the forebody. The boundary layers that are dominated by laminar or turbulent flow result in similar, large-amplitude asymmetries. If this phenomenon holds true for realistic forebodies in flight, then the Reynolds number of this test could have fallen within this reduced asymmetry region. Both the water-tunnel and the flight test Reynolds numbers appear to be well clear of this Reynolds-number range.

The wind tunnel did show that the strake pair reduced the yawing moment asymmetry, which was why the strakes were installed on the flight vehicles. In addition the tunnel test was used to predict the changes to the basic aircraft static aerodynamics caused by the strakes. This was important because several of the candidate strake designs caused undesirable changes to $C_{n\beta}$ and/or unacceptable nose-up increments to the static pitching moment, C_m. Once the field of candidate strakes was reduced to one, the impact of the strake on the overall flying qualities under realistic dynamic conditions was using the NASA Langley drop model technique.[10] Utilizing these scale-model test methods resulted in rapid acceptance of the final strake design taken to flight.

Comparison With Wind Tunnel

Ref.6

94-165
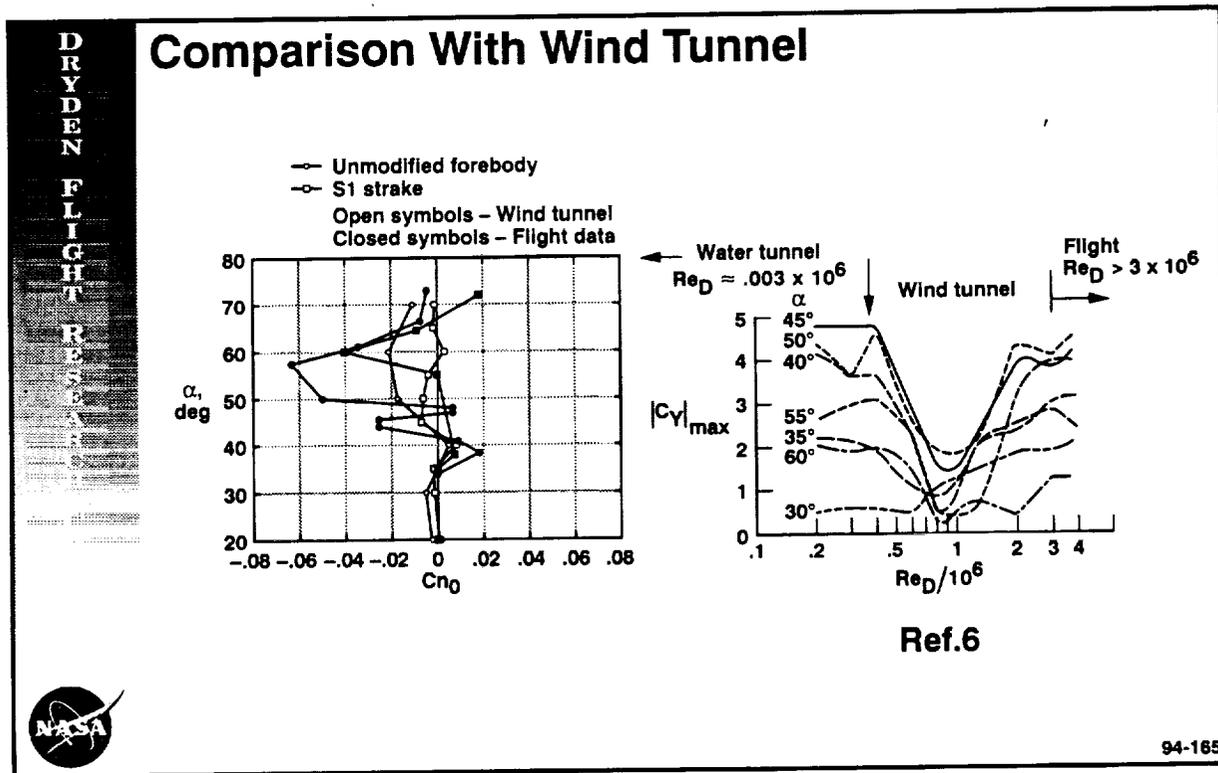
Single-Strake Test

To see what level of asymmetry could be generated on the forebody in the wind tunnel, a test was run with a strake only on one side of the forebody. A comparison of the asymmetry measured with the one-sided strake to the asymmetry measured in flight with no strake shows a reasonably good comparison, both of magnitude and of α range. The yawing moment asymmetry magnitude was slightly larger with the one-sided strake than the flight data. Thus, using a small strake to force asymmetric boundary-layer separation resulted in data that more closely matched that measured in flight. This method may have the promise of simulating a higher Reynolds-number condition to get better estimates of the asymmetries. These estimates could then be used to define control power requirements and aid in control law design.

Single-Strake Test

94-166
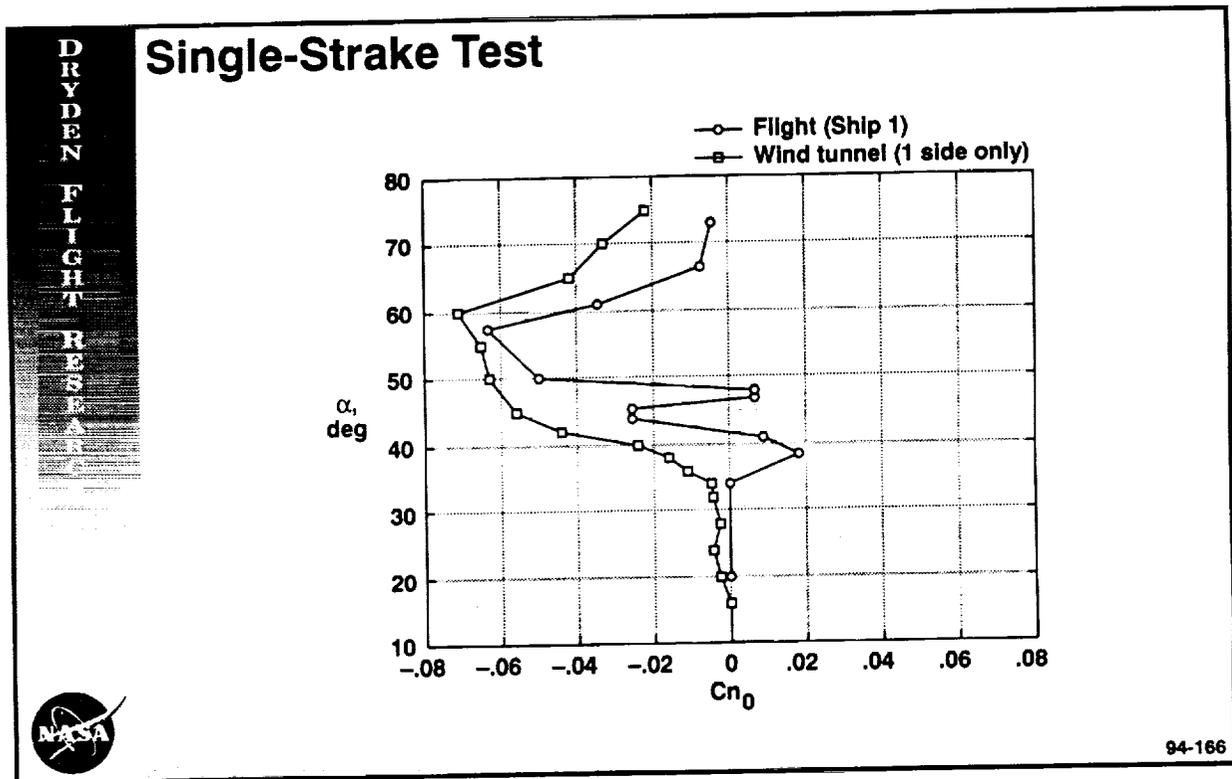
Water-Tunnel Results

Shortly before the first flight with the new forebody strakes, a water-tunnel test of a 4.4-percent scale forebody-only model of the X-31 was conducted at the NASA Dryden Flow Visualization Facility.[11] The study primarily focused on determining the relative effects of the different configurations on the stability and symmetry of the high-angle-of-attack forebody vortex flowfield. Although no force balance data were obtained, extensive flow visualization was conducted. Tests were conducted with varying strake and noseboom configurations. Notes, photographs, and video data were taken at each of the angle of-attack-conditions.

Water Tunnel Results

DRYDEN FLIGHT RESEARCH

Video: $\alpha = 60°$, $\beta = 0°$

Configuration	Strake	Noseboom
B	No	No
A	No	Yes
D	Yes	Yes
G	Yes	Modified

94-167

Although no quantitative data were taken, the water-tunnel flow visualization results compared reasonably well with the flight data. Asymmetries in the boundary layer separation and vortex cores were seen between $\alpha = 50°$ and $65°$, as was the case with the flight results. The largest deviation between the left and right vortex and boundary-layer positions was seen at $\alpha = 60°$, which is the angle of the greatest asymmetry magnitude in flight. The installation of the strakes on the model did not eliminate the asymmetry, as was the case with the flight results.

Tests without the noseboom installed were also completed to see what effect that might have. Surprisingly, no asymmetries were found at any angle of attack, regardless of the strake configuration. The unsteady wake of the noseboom appeared to be the catalyst that triggered the asymmetries to form. This oscillating wake initiated around $\alpha = 50°$. An alternative L-shaped noseboom—whose wake did not intersect the forward portion of the forebody—did not produce asymmetries in the vortex cores. A nosetip boom (similar to the X-29 noseboom) failed to improve the forebody vortex system asymmetry.

D
R
Y
D
E
N

F
L
I
G
H
T

R
E
S...

Comparison With Water Tunnel

(+) agrees   (–) disagrees

+ **Asymmetry range $\alpha = 50°$ to $65°$**

+ **Maximum asymmetry at $\alpha = 60°$**

+ **Strakes do not eliminate asymmetry (unsteadiness reduced somewhat)**

– **Strakes delay asymmetry to higher angle-of-attack (flight – yes, water tunnel – no)**

• **Flight test noseboom is primary cause of unsteady flow that caused vortex asymmetry**

• **Asymmetry eliminated with noseboom redesign or removal**

94-168

Conclusions

Flight test
- Combination of S1 forebody strakes and blunt-nose tip
  - Increased the angle-of-attack at which the asymmetry initiated by 7° to 12°
  - Reduced the maximum asymmetry
  - Made the asymmetry repeatable
- Forebody boundary layer transition strips
  - Increased the level of the yawing moment asymmetry
  - Widened the angle-of-attack range over which the asymmetries acted
  - Reduced the random asymmetry behavior of the unmodified forebody on Ship 2
- Noseboom boundary-layer transition strips
  - Ensured that a turbulent separation existed on the noseboom, thereby minimizing the noseboom wake
  - The S2 strakes reduced the additional asymmetry present during dynamic maneuvers (Ship 2)

94-169

Conclusions

Wind tunnel
- Showed that strakes reduced the asymmetry
- Predicted asymmetry angle-of-attack range, but did not predict yawing moment asymmetry magnitude
- Separating boundary layer on one side resulted in asymmetry magnitudes near flight

Water tunnel
- Qualitatively predicted the asymmetry angle-of-attack range and the angle of maximum asymmetry
- Showed noseboom position is a catalyst for asymmetric condition
- Alternate or removal of noseboom eliminates asymmetry

94-170

Current Flight Status

The combination of the forebody strakes, rounded nosetip, noseboom grit, increased thrust vector vane travel (from 26° to 35°), and minor control law changes has allowed the elevated-g envelope expansion out to about 5.5-g entry conditions to be completed on ship 1. An 8-in. strake extension combined with a further blunting of the X-31 nosetip have allowed the same envelope to be completed on ship 2 as well. Although some asymmetry still exists, enough control power is available to coordinate maneuvering. Once maximum afterburner is set, the X-31 has been cleared for all stick inputs at all angles of attack—essentially carefree handling. The pilots have reported good handling qualities throughout the high-α envelope. Typical high-α combat maneuvering results in sideslip values less than 3°.

D R Y D E N   F L I G H T   R E S E A R C H

Current Flight Status

- **Strake, rounded nosetip, noseboom grit, and increased thrust vector vane travel allowed Ship 1 to complete envelope expansion**

- **After increasing strake length by 8 in. and increasing nose radius, Ship 2 completed envelope expansion**

- **Current envelope**
    - **$\alpha < 30°$, 6-g maximum**
    - **$\alpha > 30°$, 265 KCAS (M = 0.7, 30k)**
    - **Maximum afterburner above $\alpha = 30°$**
    - **No limitation on pilot input ("carefree handling")**
    - **p-stab > 40 deg/sec, $\beta < 3°$**

- **No restrictions on tactical utility**

94-171

References

1. Keener, Earl P., Gary T. Chapman, Lee Cohen, and Jamshid Taleghani, *Side Forces on a Tangent Ogive Forebody with a Fineness Ratio of 3.5 at High Angles of Attack and Mach Numbers from .1 to .7*, NASA TM X-3437, 1977.

2. Lamont, P. J., "Pressure Measurements on an Ogive-Cylinder at High Angles of Attack With Laminar, Transitional, or Turbulent Separation," AIAA-80-1556, Jan. 1980.

3. Moskovitz, C., R. Hall, and F. DeJarnette, "Experimental Investigation of a New Device to Control the Asymmetric Flowfield on Forebodies at Large Angles of Attack," AIAA-90-0069, 28th Aerospace Sciences Meeting, Reno, NV, Jan. 8–11, 1990.

4. Chapman G. T., Keener E. R., Malcolm G. N., "Asymmetric Aerodynamic Forces on Aircraft Forebodies at High Angle of Attack—Some Design Guides," AGARD CP-199, Nov. 1975.

5. Kruse, Robert L., Earl R. Keener, Gary T. Chapman, and Gary Claser, *Investigation of the Asymmetric Aerodynamic Characteristics of Cylindrical Bodies of Revolution With Variations in Nose Geometry and Rotational Orientation at Angles of Attack to 58° and Mach Numbers to 2*, NASA TM-78533, 1979.

6. Lamont, P. J., "The Complex Asymmetric Flow Over a 3.5D Ogive Nose and Cylindrical Afterbody at High Angles of Attack," AIAA-82-0053, 20th Aerospace Sciences Meeting, Orlando, FL, Jan. 11–14, 1982.

7. Fisher, David F. and Brent R. Cobleigh, "Controlling Forebody Asymmetries In-Flight-Experience with Boundary Layer Transition Strips," AIAA-94-1826, Applied Aerodynamics Conference, June 20, 1994.

8. Cobleigh, Brent R., "High-Angle-of-Attack Yawing Moment Asymmetry of the X-31 Aircraft from Flight Test," AIAA-94-1803, Applied Aerodynamics Conference, June 20, 1994.

9. Shevell, Richard S., *Fundamentals of Flight*, Prentice-Hall Inc., Englewood Cliffs, NJ, 1983.

10. Croom, Mark A., David J. Fratello, Raymond D. Whipple, Matthew J. O'Rourke, and Todd W. Trilling, "Dynamic Model Testing of the X-31 Configuration for High Angle of Attack Flight Dynamics Research," AIAA-93-3674, Flight Mechanics Conference, Monterey, CA, Aug. 9-11, 1993.

11. Cobleigh, Brent R., *Water-Tunnel Flow Visualization Study of a 4.4-Percent Scale X-31 Forebody*, NASA TM-104276, 1994.